Molecular Physics
Vol. 110, Nos. 15–16, 10–20 August 2012, 1757–1766

Taylor & Francis
Taylor & Francis Group

INVITED ARTICLE

Cooling molecules in a cell for FTMW spectroscopy

David Patterson* and John M. Doyle

Harvard University, Cambridge, MA, USA

(*Received 14 January 2012; final version received 16 March 2012*)

Gas phase benzonitrile, acetone, 1-2 propanediol, fluorobenzene, and anisole molecules are produced in a cell at a temperature of 8 K, and detected via Fourier transform microwave spectroscopy (FTMW). Helium buffer gas is used to cool the molecules originating from a high flux room temperature beam. This general, continuous source of cold molecules offers comparable spectral resolution to existing seeded pulsed supersonic beam/FTMW spectroscopy experiments but with higher number sensitivity. It is also an attractive tool for quantitative studies of cold molecule–helium and molecule–molecule elastic and inelastic collisions. Preliminary data on helium–molecule low temperature rotational and vibrational relaxation cross-sections are presented. Applications of the technique as a sensitive broad spectrum mixture analyser and a high resolution slow-beam spectrometer are discussed.

Keywords: molecular spectroscopy; buffer gas cooling; Fourier transform microwave spectroscopy

1. Introduction

In 1974, Smalley *et al*. revolutionized modern physical chemistry by demonstrating the first seeded supersonic jet [1]. In early experiments they cooled molecules as diverse as I_2, $C_2H_2N_4$, and NO_2 to less than 1 K in a supersonic moving frame, detecting them via laser-induced fluorescence. Since that pioneering work, seeded supersonic jets have become a workhorse of high precision spectroscopy, following especially the work of Balle and Flygare who combined the supersonic jet with high resolution microwave Fourier transform spectroscopy (FTMW) [2]. The low temperatures (rotational 1–5 K typical and translational 1–2 K typical in the moving frame) in seeded supersonic jets make them particularly attractive as cold sources of larger molecules. At room temperature these molecules typically occupy many thousands of rovibrational states, making spectroscopy challenging at best and in many cases impossible; cooling leads to substantial population enhancement of lower rotational states and a dramatic simplification of the spectrum. Dudley Herschbach played a pivotal role in the early development of these beams, creating early unseeded [3] and seeded [4] beams prior to Levy's work, as well as numerous studies and applications of later seeded molecular beams [5,6]. It is an honor to present this new source of cold molecules in a festschrift for Dr. Herschbach.

In recent years significant progress has been made developing new sources of cold and ultracold *small* molecules, including buffer gas cooling [7], laser cooling [8,9], photoassociation [10] and magnetoassociation [11]. Due to the large number of degrees of freedom all of these methods except buffer gas cooling are currently infeasible for molecules with more than two atoms. Buffer gas cooling has previously been used to produce cold samples of molecules with 2–5 atoms [12]. Our earlier buffer gas cooling experiments [13] and seeded supersonic jets are the only previously demonstrated source of larger (>5 atoms) cold molecules.

Here we cool and detect five different large molecules to demonstrate a robust, general method for producing continuous, high densities of larger cold molecules via buffer gas cooling. The helium density in this work ($\approx 10^{14}$ He cm^{-3}) is dramatically lower than in our previously demonstrated buffer gas sources of larger cold molecules [13]. This relatively low-collision environment allows the molecules to be detected via FTMW spectroscopy with linewidths of 20–200 kHz, and opens the door to producing cold, slow, continuous beams of these molecules for high resolution

*Corresponding author. Email: dave@cua.harvard.edu

ISSN 0026–8976 print/ISSN 1362–3028 online

http://dx.doi.org/10.1080/00268976.2012.679632
http://www.tandfonline.com

spectroscopy or further slowing and trapping experiments.

2. Experimental

The basic idea behind our approach is to inject warm molecules into a buffer gas cell while keeping to an absolute minimum the parasitic heat loads on the buffer gas in the cell. Earlier gas-phase buffer gas cooling experiments used laser ablation [7] or warm capillaries [14,15] to inject gas phase molecules into a cold helium buffer gas. These methods are effective, but end up depositing far more heat from parasitic heat loads (e.g. helium atoms colliding with a hot capillary) than from the hot molecules themselves. In this work, which is heavily informed by earlier work on cooling and trapping NH and atomic nitrogen [16], we have placed the hot beam source outside but close to the cell, all but eliminating thermal contact between the hot injection line and the cold vapour in the cell. This disconnect allows us to make the injection tube substantially hotter and larger than any reasonable in-cell capillary.

Figure 1 shows the low temperature portion of the experimental apparatus. A hot (300 K, 0.5 cm diameter) injection tube is held ≈2 cm away from a circular aperture (1.25 cm diameter) in a cold cell (7–12 K, 8 cm × 8 cm × 8 cm), which is anchored to the cold stage of a commercial pulse tube refrigerator. Aluminized mylar superinsulation around the warm injection tube reduces the radiative heat load on the cell to ≈1.5 watts. Cold (7 K) 0.2 cm diameter fill lines deliver helium gas either to an annular manifold around the aperture [Figure 1(b)] or to an intake manifold on the opposite side of the cell [Figure 1(a)].

A large flow [typically 2×10^{18} molecule s^{-1}, or 3 sccm (standard $cm^3\,min^{-1}$)] of warm molecules exits the tube and flies ballistically towards the cell. As the molecules travel, they collide with helium atoms exiting the cell. The collisions both cool and slow the incoming molecules. Since almost all molecules have a mass significantly larger than that of the helium buffer gas atoms, it takes many (≈20) collisions to fully thermalize a hot molecule. Our simple model is that the molecules fly more or less ballistically through the counterpropagating helium cloud until they are within the cell. Simulations back up this simple picture and suggest 10–20% of the molecules emitted from the hot tube end up thermalized within the cell, the fraction being set approximately by the solid angle of the aperture as seen from the injection tube. The flow rate of cold helium is tuned to a level high enough to give the molecules an in-cell diffusion time of a few ms, but low enough that molecules are not stopped close to the aperture, where they would be pushed away from the cell and lost. In practice this helium flow rate falls in the range of 2–8 sccm, and the molecule free induction decay signal strength is only moderately sensitive to variations in the helium flow rate.

Once molecules enter the cell, they continue to thermalize with the cold helium gas, which in turn thermalizes with the cell walls. As in [13], at this stage two competing processes are at work in the cell. (1) Molecules diffuse to the cold cell walls, where they freeze and are lost from the experiment. (2) Heat diffuses to the walls, where the helium buffer gas is cooled to the cell temperature of ≈7 K by absorption and desorption. Both simulations and experimental data suggest that the thermalization process is substantially more rapid than diffusion. This is to be expected for any molecule $\mathcal{X}$ such that the helium–$\mathcal{X}$ total cross-section is even modestly larger than the helium–helium elastic cross-section, which is likely true for essentially all molecules.

2.1. *Molecule detection*

Cold molecules are detected via FTMW spectroscopy, using a technique very similar to the room temperature static gas waveguide experiments of Balle and co-workers [17]. Figure 2 shows the microwave circuit.

Unlike most pulsed supersonic sources, this is a continuous source; the microwave pulse/detect sequence can be repeated essentially as fast as the rotational rethermalization rate. Our current system can record narrow band (10 MHz) spectra of pure chemicals with a SNR of >500 in about 30 s of integration time, which is heavily dominated by dead time in our current (first generation) data acquisition system (a Tektronix TDS2054 oscilliscope). The next generation will include a dedicated 350 MHz bandwidth signal averager with negligible dead time (Agilent U1084A), reducing experimental runtimes by a factor of more than 100.

It should be emphasized that although our current microwave electronics allow us to excite and digitize only a narrow (≈10 MHz) portion of the spectrum at a time, the hardware is fundamentally *broadband*. In particular, there should be no degradation of signal, and an enormous gain in bandwidth, in moving to a chirped-pulse FTMW setup, capable of digitizing large portions of the microwave spectrum in a single pulse [18].

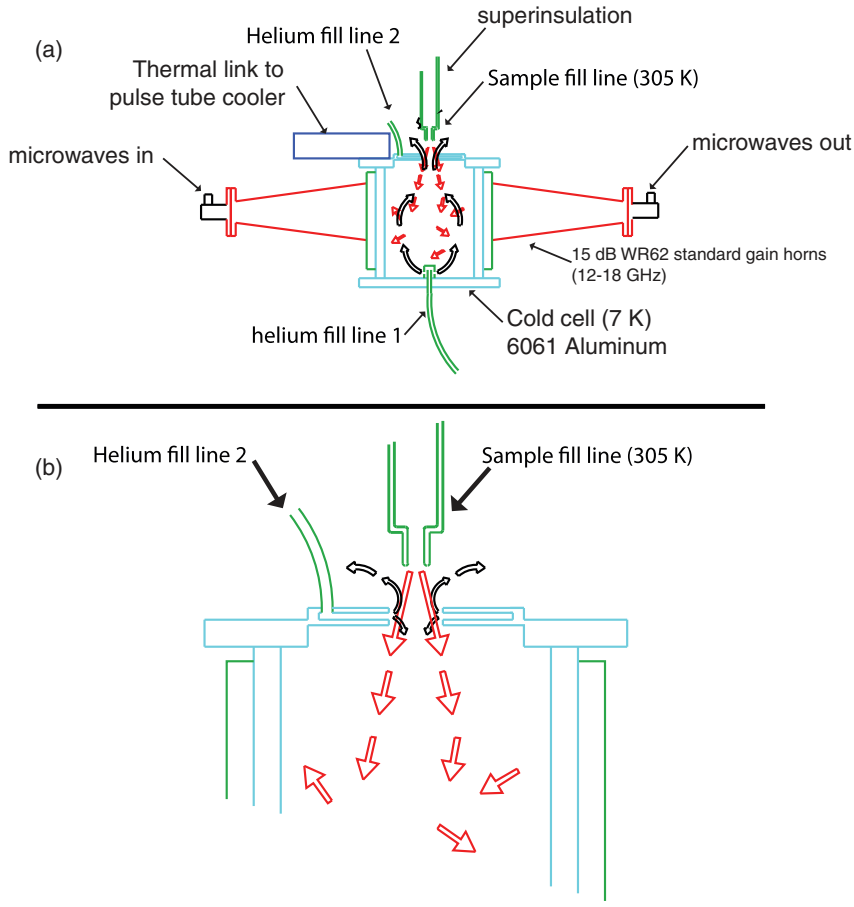

Figure 1. Schematic of the low temperature cell and microwave hardware. Molecules are sprayed through a warm (305 K) injection tube into a counterflowing stream of cold helium atoms. A significant fraction of the molecules enter the cold cell, where they thermalize and eventually diffuse to the cold cell walls and freeze. The resulting translationally and rotationally cold gas is polarized by a brief, strong microwave pulse (≈100 ns, 300 mW), and the resulting free induction decay is collected by a second microwave horn, amplified, mixed down to ≈10 MHz, and digitized. Cold helium gas can be introduced into the cell from either of two fill lines. In (a), the helium is introduced via a fill line entering the back of the cell. In (b), the gas is introduced via an annular slit surrounding the aperture. This second geometry reduces the helium density and helium 'wind' speed inside the cell. Signal strengths were comparable with the two geometries; most data presented in this paper was taken under geometry (b).

3. Results

We used our apparatus to cool and detect five different molecules: benzonitrile, acetone, 1-2 propanediol, fluorobenzene, and anisole. Figure 3 shows a typical trace of a FID signal from cold (8 K) 1-2 propanediol, on the $1_{01} \Rightarrow 2_{02}$ transition of the ground state conformer. This trace represents 15,000 averages, or about 30 s of experiment time. The best estimates for conditions during this pulse are 1-2 propanediol total density $n = 2 \times 10^{12}\,\mathrm{cm}^{-3}$, helium density $n_{\mathrm{He}} = 2 \times 10^{14}\,\mathrm{cm}^{-3}$, temperature $T = 7.5\,\mathrm{K}$, total radiated microwave power 6 picowatts (−82 dBm)[1]. This radiated power is about 400 times lower than predicted [17]. We believe this factor is at least partially due to the poor microwave mode quality transmitted through the cell. In such a situation only a small fraction of the molecules feel a '$\pi/2$' pulse for any given polarization pulse, and much of the resulting FID signal is not coupled to the detected output channel.

Figure 4 shows the amplitude of the $0_{00} \Rightarrow 1_{11}$ transition in acetone at 15,074.1 MHz as a function of cell temperature. The predicted scaling as $T^{-5/2}$ is shown for comparison [19]. The signal in fact seems to grow as $T^{-7/2}$, regardless of which molecule or rotational transition was observed. The most probable explanation for this difference is that the diffusion time and hence the molecule density in the cell also vary as T^{-1}. At lower temperatures, the molecules diffuse more slowly as a result of a slower molecular thermal velocity. In addition, the helium density in the cell

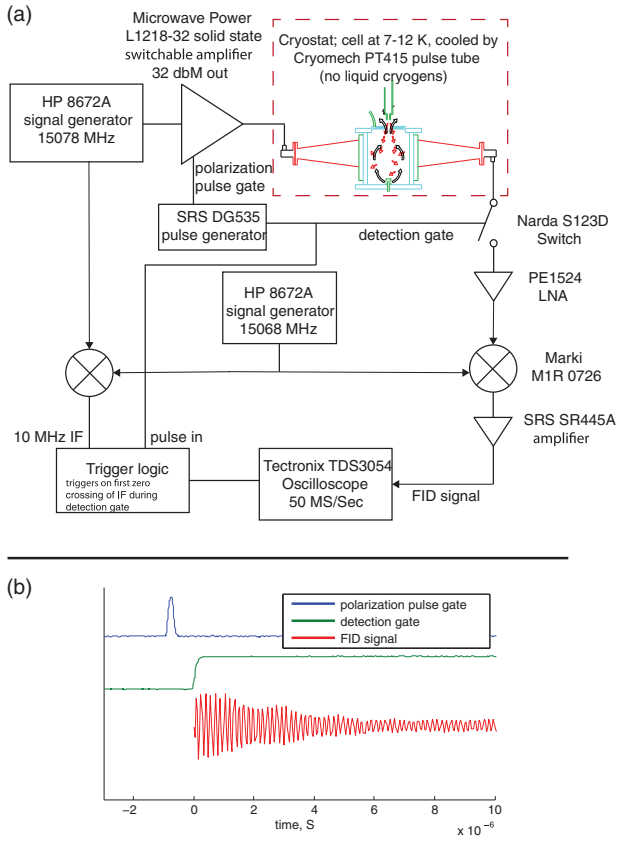

Figure 2. (a) Schematic of the FTMW spectroscopy apparatus. A brief (typically 100 ns) powerful (typically 0.3 watt) microwave pulse is produced by a switchable solid-state amplifier (AML L1218-32) and directed into the cell via a 15 dB gain (4 cm × 6 cm) microwave horn. This pulse gives the molecular gas a macroscopic oscillating dipole moment; radiation from this oscillating dipole is collected by a second 15 dB horn, amplified, downconverted to ≈10 MHz, and digitized. A fast RF switch (Narda S123D) protects the low noise amplifier from damage from the polarization pulse. Under typical conditions, the lifetime of the free induction decay signal is limited by helium–molecule inelastic collisions. Frequency values are typical values for detecting the 15,074.1 MHz transition in acetone. (b) A typical timing diagram, showing the polarization pulse gate, the detection gate, and the averaged FID signal from cold benzonitrile.

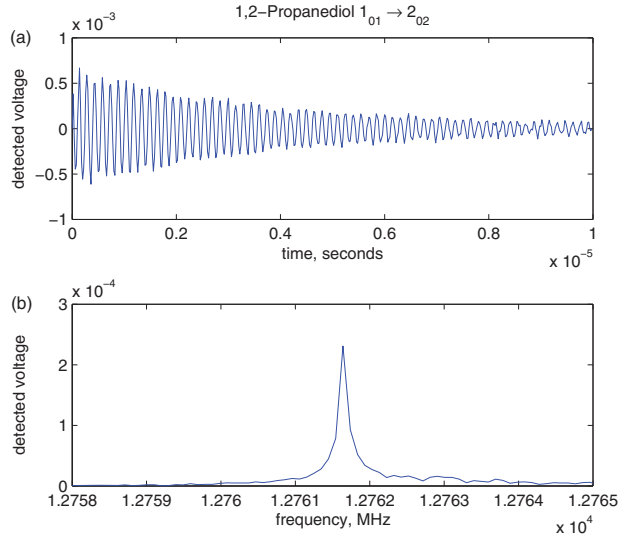

Figure 3. The FID signal of 1,2 propanediol, lowest energy conformer, $1_{01} \Rightarrow 2_{02}$ at 7.5 K. (a) The time domain signal. This signal represents 15,000 averages, or about 30 s worth of real time data acquisition. Our experimental repetition rate is strongly limited by our data acquisition system; this data represents only 200 ms worth of actual integration. (b) The Fourier transform, clearly showing the expected peak at 12,761.6 MHz.

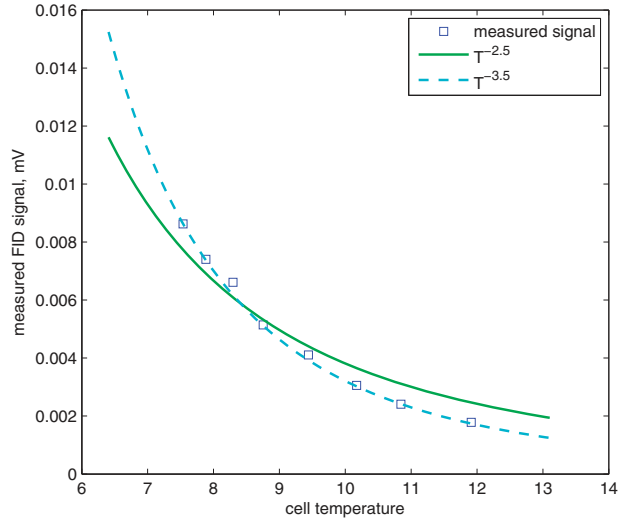

Figure 4. The measured acetone FID signal as a function of cell temperature, as measured by a diode thermometer on the outside of the cell. At a constant molecule density the measured voltage is expected to vary as $T^{-5/2}$. The faster variation here suggests that the total density of molecules also rises as the temperature drops.

increases if the helium flow rate is held constant and the temperature is lowered, further increasing molecular diffusion times. Large signal amplitude fluctuations with microwave frequency due to the complex mode structure of our first generation cell make it difficult to extract meaningful rotational temperatures even from molecules with several observed lines, but the observed dependence on temperature provides strong indirect evidence that the molecules are in fact close to equilibrium with the cold cell walls.

Figure 4 strongly suggests that our signal would benefit substantially from a lower cell temperature. Parasitic heat loads, most notably poorly controlled blackbody radiation, currently limit our cell

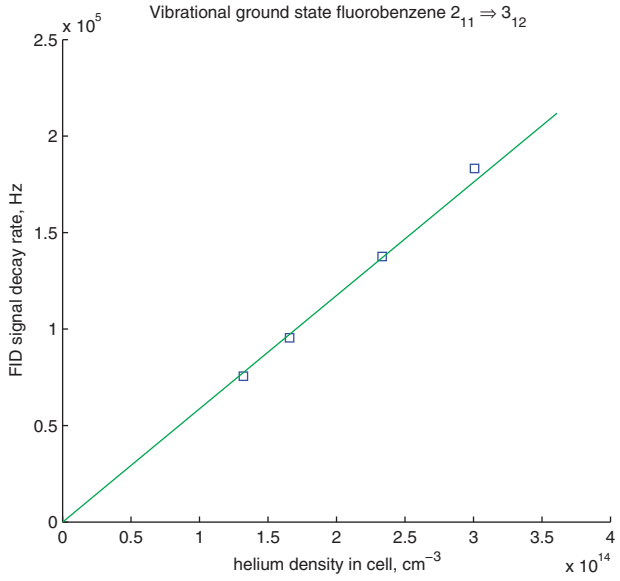

Figure 5. The measured decay rate (blue squares) of the free induction decay signal of fluorobenzine as a function of helium density. The linear scaling with helium density is expected in the case where collisional broadening is dominant. The line shows the expected decay rate for a $\sigma_{\text{inelastic}} = 2.9 \times 10^{-14}\,\text{cm}^2$.

temperature to 7 K or above, but it should be straightforward to extend this down to about 3 K with minimal hardware changes, and possibly ≈1 K in an optimized system.

3.1. *Inelastic scattering*

We have measured rotational inelastic cross-sections for collisions between helium and acetone, fluorobenzene, and several conformers of 1-2 propanediol. Figure 5 shows the decay rate of the free induction signal of the $2_{11} \Rightarrow 3_{12}$ transition of fluorobenzene as a function of helium gas density. The signal decay rate scales almost linearly with helium density, as would be expected if collisional broadening was dominant. The combination of the measured decay rate and the known helium density and temperature yield an inelastic rotational relaxation cross-section, in this case $\sigma_{\text{inelastic}} = 2.9 \times 10^{-14}\,\text{cm}^2$.

The FID signal is expected to decay according to

$$S(t) \propto \exp(-t/T_1)\exp[-(t/T_2)]\cos(\omega_0 t), \qquad (1)$$

where T_1 describes the rate of thermal relaxation of level populations, and T_2 describes dephasing, in this case from collisions with background helium atoms that change the phase of the molecule but not the state. In a semi-classical picture, T_1 describes the rate of collisions which change the angular momentum of the molecule, and T_2 describes the rate of collisions which leave the angular momentum unchanged, but reorient the molecular axis. A typical rethermalization collision takes the molecule from one of the two states involved in the FID to one of a potentially large number of nearby states. As the molecule gets larger, this simple picture would indicate that T_1 will decrease while T_2 will remain unchanged, as more and more nearby rotational states become available.

On the Bloch sphere, these two processes can be seen as returning the polarization vector to the south pole (thermal relaxation, T_1), or distributing the vector around the equator of the sphere (decoherence, T_2). It is clear from the form of Equation (1) that it is not possible to tell from a FID signal alone whether or not the observed decay comes from state population relaxation or from dephasing. However, if dephasing were the dominant process, a rapid repeat of the experiment after time t, where $T_1 > t > T_2$, would result in a substantially smaller signal, as a $\pi/2$ pulse applied to molecules distributed at random on the equator of the Bloch sphere would not result in a macroscopic polarization. No such decrease is found, and so we tentatively conclude that $T_1 \lesssim T_2$, as seen in room temperature experiments and in agreement with the simple semiclassical argument above [17,20].

Table 1 shows the measured 8 K helium–$\mathcal{X}$ inelastic rotational cross-section for various transitions in various species. The cross-sections vary modestly with molecule, conformal state, and rotational state. Groner *et al.* have seen similar but smaller variation in room temperature experiments [21]. Such variations are expected to increase with decreasing temperature, as fewer energetically allowed channels and fewer partial waves are involved in the collision [14]. Rotational relaxation cross-sections for larger (>5) atoms have not previously been measured, but the values in Table 1 are a factor of 5–10 larger than low temperature rotational relaxation cross-sections of H_2CO and CH_3F previously measured via collisional broadening in mm-wave absorption spectroscopy [12,22].

3.2. *Molecule density*

At present we have no reliable direct measurement of the molecule density or the total number of cold molecules in the cell. Under the assumption that the dominant loss mechanism in the cell is diffusion to the cold walls, and that the molecule–helium elastic collision rate is comparable to the measured molecule–helium inelastic collision rate of ≈100 kHz, the

Table 1. Preliminary molecule–helium inelastic cross-sections for a representative sample of molecules and states. The measured cross-sections are all significantly larger than the He–He elastic cross-section at this temperature of $5 \times 10^{-15}\,\mathrm{cm}^2$ [26]. In the current work we cannot resolve individual state-specific cross-sections, and the cross-sections listed are the sum of all 'thermalization' inelastic channels connecting the two states in the transition to each other or to other states. MW-MW or IR-MW double resonance experiments could resolve individual component cross-sections. Conformer labels are from [33]. Absolute cross-sections are accurate to within 50%, with the uncertainty dominated by uncertainty in the helium gas density and temperature; relative cross-sections are accurate to 10%.

Species	Transition	σ (cm^2)
1-2 Propanediol Conformer 2	$1_{01} \Rightarrow 2_{02}$	5.2×10^{-14}
1-2 Propanediol Conformer 3	$1_{01} \Rightarrow 2_{02}$	4.6×10^{-14}
1-2 Propanediol Conformer 3	$3_{12} \Rightarrow 4_{04}$	3.8×10^{-14}
Fluorobenzine	$2_{11} \Rightarrow 3_{12}$	2.8×10^{-14}
Acetone	Torsional state Q, $0_{00} \Rightarrow 1_{11}$	2.6×10^{-14}

diffusion time of a molecule to the cell walls is calculated to be about 5 ms. This is consistent with the directly measured diffusion time of NH in similar cold buffer gas cells [23]. This diffusion time, combined with a calculated input flux of 2×10^{17} molecule s^{-1} implies a total molecule number $N \approx 1 \times 10^{15}$, and a mean density of $n_{\mathrm{molecule}} \approx 2 \times 10^{12}$ molecule cm^{-3}, which we take as a reasonable order of magnitude estimate.

It is *a priori* possible that molecule–molecule clustering is the dominant loss mechanism for monomer molecules in the cell. Several pieces of evidence suggest this is not the case. The FID signal continues to increase approximately linearly with molecule input flux even at fluxes significantly beyond the nominal conditions presented here. In addition, adding a substantially larger flux of a second molecule, e.g. water, does not significantly effect the FID signal of monomer benzonitrile. We have also looked directly for the FID signature of some simple complexes which have been observed in supersonic jets, such as benzonitrile $\cdot$ H_2O and $(CH_3OH)_2$ [24,25]. We detected no complexes, and can place an upper bound on the density of such complexes at 1% of typical monomer densities. Under the conditions described in the previous paragraph, a typical molecule would collide on the order of 10 times with other cold molecules before freezing to the walls. Two-body 'clustering' cross-sections for large molecules are also unknown; this data therefore suggests that these two-body cross-sections are at least order of unity smaller than elastic cross-sections. Evidence of molecule–molecule clustering at similar molecular densities was seen in earlier buffer gas cooling work with naphthalene, in a much higher density helium gas ($n_{\mathrm{He}} \approx 10^{17}\,\mathrm{cm}^{-3}$) [13,26]. This discrepancy suggests that the 'two-body' recombination $\mathcal{X} + \mathcal{X} \Rightarrow \mathcal{X}_2$ observed in that work was in fact mediated by a third body, $\mathcal{X} + \mathcal{X} + \mathrm{He} \Rightarrow \mathcal{X}_2 + \mathrm{He}$. The three-body channel is suppressed in the current work by the much lower helium density.

3.3. *Vibrational modes and conformers*

Inelastic molecule–helium vibrational relaxation cross-sections are typically dramatically smaller than rotational relaxation cross-sections [27,28]. The vibrational temperature of molecules in a supersonic expansion is far less predictable and typically substantially higher than the rotational and translational temperatures – a phenomenon that was indeed first explored by Herschbach [29,30]. Although both inelastic and elastic molecule–carrier gas collisions play important roles in supersonic jets, these collisions take place in the rapidly changing and poorly controlled environment very close to the nozzle itself, making quantitative measurements all but impossible. In supersonic jets molecules experience thousands of 'warm' collisions at intermediate temperatures in the first few nozzle diameters, and very few collisions at low temperatures. The situation here is exactly the reverse: molecules in our buffer gas source experience hundreds or thousands of cold ($< 10\,\mathrm{K}$) collisions with helium atoms and very few (< 10) collisions at higher energies ($> 100\,\mathrm{K}$).

Figure 6(a) shows the spectrum of buffer gas cooled fluorobenzene in the neighbourhood of its $2_{11} \Rightarrow 3_{12}$ transition at 14,125.5 MHz. Several satellite peaks, corresponding to known vibrationally excited states of fluorobenzene, are clearly observable [31]. Figure 6(b) shows the relative concentration of ground state and vibrationally excited fluorobenzene as a function of helium density; at higher densities, the fraction of excited molecules clearly drops, as the molecules thermalize via inelastic collisions with the cold helium gas. The relaxation rate varies significantly with vibrational state; our estimates of the $\mathrm{FBn}_a + \mathrm{He} \Rightarrow \mathrm{FBn}_0$ cross-section range from 5×10^{-17} to $5 \times 10^{-15}\,\mathrm{cm}^2$, depending on the vibrational state. To our knowledge low temperature vibrational relaxation cross-sections for such large molecules have not been calculated theoretically. Theoretical predictions of low temperature He–CO inelastic cross-sections are consistent with our results to within an order of magnitude [32].

Non-ground state conformers of 1-2 propanediol with energies in the 100–200 K range were also been

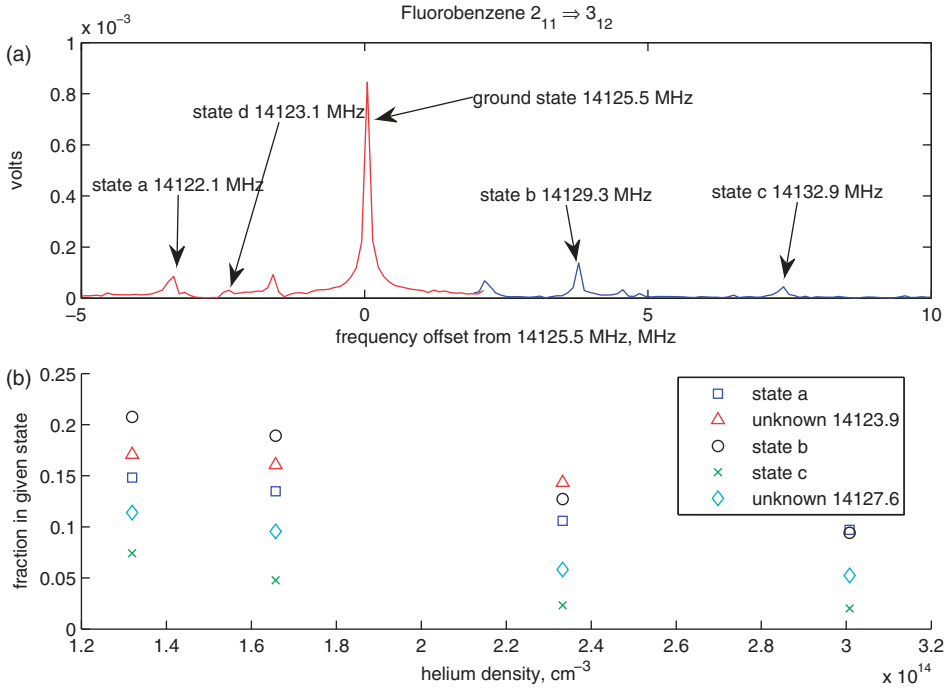

Figure 6. (a) The FTMW spectrum in the neighbourhood of the $2_{11} \Rightarrow 3_{12}$ transition in fluorobenzene. The ground vibrational state and several satellite peaks can be seen. Peaks are labelled following the tentative identifications in [31]; the two unlabelled peaks have not been identified, but have also been observed in supersonic expansions. (b) The relative population of various vibrationally excited states compared to the ground state population as a function of helium density. The decreasing vibrationally excited population at high density is indicative of thermalization as the molecules undergo collisions in the cell. The spectrum shown is actually a combination of spectra taken separately (shown in red and blue), due to our limited digitization bandwidth.

observed, as in supersonic jets [33]. Signals from torsionally excited states of acetone with similar energies of 80 and 125 cm^{-1} were not observed, suggesting that this degree of freedom thermalizes rapidly [34].

4. Applications

4.1. *Buffer gas cooling as a chemical mixture analyser*

There are numerous proposals (see for example US Patent 5831439) and demonstrations [35] of supersonic beams as chemical analysers and trace gas detectors [36]. In particular, the combination of a supersonic source with microwave or mm wave FTMW detection can provide a general, sensitive detector that can detect trace quantities (ppb under favourable conditions) of almost any polar molecule. Such proposals have become particularly attractive with the recent development of broadband chirped-pulse FTMW techniques [18], which take advantage of modern broadband synthesizers and digitizers to record large sections of the microwave spectrum simultaneously. Chirped pulse FTMW techniques, which are entirely compatible with the high density, continuous source demonstrated in this work, have recently been used to detect biomolecules with as many as 29 atoms such as strawberry aldehyde [37], nicotine [38], and phenylalanine [39]. Such an instrument can provide rapid, sensitive detection of thousands of chemical species simultaneously, and with the incorporation of microwave–microwave or microwave–infrared double resonance techniques could offer unparalleled specificity, allowing trace compounds to be identified amid a complex chemical background. It is therefore natural to consider a similar analyser based on the high-density continuous buffer gas source presented here.

A useful figure of merit for comparing the sensitivities of different spectroscopic instruments is $F = NT^{-5/2}R^{1/2}$, where N is the total number of molecules being interrogated by a given pulse sequence, T is the rotational temperature of the molecules, and R is the maximum realizable experimental repetition rate. Given similar microwave electronics, the signal to noise of the instrument, and thus the lowest detectable concentration of a given component, will scale linearly with F.[2] Table 2 shows

Table 2. Estimated total number N, rotational temperature T, physically realizable repetition rate R, and spectrometer sensitivity figure of merit $F^* = 1.210_{14}F = 1.210_{14}NT^{-5/2}R^{1/2}$ for the source presented in this work and FTMW spectrometers based on pulsed supersonic beams. The 50 kHz R value has been realized since this work was originally submitted with an updated DAQ system based on the Agilent U1084 signal averager.

Type	N	T (K)	R (Hz)	$F^* = 1.2 \times 10^{-14} NT^{-5/2}R^{1/2}$
Seeded free jet expansion [40]	10^{14}	1–2 typical	20	1
Buffer gas source	10^{15}	5	50,000	50

estimated N, T, R, and a scaled F, F^* for both technologies.

It is clear that even our first generation source could have substantially more sensitivity than current state of the art pulsed supersonic source spectrometers. Further improvements, most notably a reduction in T, could significantly improve our sensitivity.[3] Our microwave electronics are crude compared to mature FTMW trace gas analysers, but could be improved in future generations of the experiment.

An important question for the application of this technique as a trace gas detector or mixture analyser is the applicability of this technique to still larger molecules, such as hormones and other small biomolecules. The upper size limit for molecules which can be buffer gas cooled without adsorbing one or more helium atoms remains unknown, due to uncertainty about the efficacy of molecule–He two- and three-body clustering for molecules with many energetically accessible vibrational degrees of freedom [13]. It should be noted that many larger molecules lack sufficient vapour pressure at room temperature to produce the high fluxes required by this technique; we have recently demonstrated an improved version of the device demonstrated here with a lower cell temperature (5 K) and a modestly warmer (400 K) injection tube, allowing us to detect larger, less volatile species such as the polycyclic aromatic hydrocarbon fluorene ($C_{13}H_{10}$).

4.2. *A buffer gas based source for high resolution spectroscopy*

With the helium density tuned to maximize sensitivity, typical FID decay rates are about 100 kHz. Spectral resolution as fine as 20 kHz has been measured in acetone spectra with the current apparatus operating at a lower helium density, and in an optimized geometry a resolution of < 10 kHz should be achievable in a buffer gas cell.

This spectroscopic resolution is significantly lower than current state-of-the-art experiments done in modern coaxial seeded-jet FTMW spectrometers (1–5 kHz typical). A higher resolution could be achieved by intentionally allowing a portion of the molecular gas/helium mixture to escape through a second aperture in the back of the cell, realizing a cold, slow, collision-free continuous beam [41]. A proposed apparatus for such a beam is shown in Figure 7. Such a beam would likely have a rotational temperature of a few K, a continuous flux of $\phi \approx 10^{15}$ molecule s^{-1}, a mean velocity of $\bar{v} \approx 100$ m s^{-1}, and a beam solid angle of $\Omega \approx 0.1$ steradian due to the mass mismatch between the molecules and helium atoms [41]. The $\bar{v} \approx 100$ m s^{-1} velocity – substantially slower than any room temperature supersonic beam – would result in longer interaction times and ultimately higher spectral resolution than current state-of-the-art COBRA spectrometers [36,42]; the ultimate resolution of such an instrument would be set by time-of-flight broadening

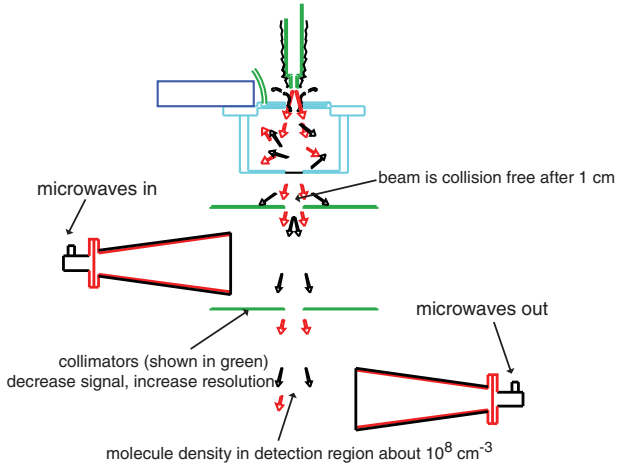

Figure 7. A proposed apparatus for performing high resolution spectroscopy on a cold, slow beam of larger molecules. Such a beam would have a forward velocity of about 100 m s^{-1}, a rotational temperature of a few K, and flux of $\phi \approx 10^{15}$ molecule s^{-1}. The low temperature and forward velocity of such a beam would reduce time-of-flight broadening (including Doppler broadening), allowing a spectral resolution of ≈200 Hz. The broadband horns shown could be replaced by cavities for higher sensitivity at the expense of bandwidth.

at about 200 Hz for a 1 m apparatus. The beam could also be an attractive source for alternating gradient Stark decelerators for large molecules [43].

5. Conclusion

We have detected FTMW signals from cold samples of benzonitrile, fluorobenzene, acetone, 1-2 propanediol, anisole, and fluorene. This breadth of success supports our contention that the technique is general and can produce cold, gas-phase samples of any molecule in this size range. The source offers experimental access to previously inaccessible collisional physics, and could potentially be the core element in microwave spectrometers of unprecedented sensitivity and spectral resolution. Preliminary measurements were made of molecule–helium inelastic rotational and vibrational relaxation cross-sections.

Notes

1. The helium density is estimated from the known helium flow rate, temperature, and cell geometry; direct measurement of helium densities in similar geometries and flow regimes have confirmed that this calculation is accurate to within 30% [44].
2. This is only true in the 'high temperature limit', where the spectrometer central frequency $\hbar\omega < k_B T$; below this temperature to noise scales as $F = NT^{-3/2}R^{1/2}$. For the 12–18 GHz band used here, the high temperature limit is applicable for any $T \gtrsim 1\,\mathrm{K}$.
3. In both our work and many supersonic beam experiments the total molecule number N is poorly quantified. Our steady state density is estimated at $n = 10^{12}$, and total number at $N = 10^{15}$. A typical 'bright' seeded supersonic source has a total $N = 1 \times 10^{15}$ molecules pulse^{-1}, spread over a 500 µs pulse and moving at $\approx 1000\,\mathrm{m\,s^{-1}}$. Taking [18] as a typical example, the molecules are interrogated as they cross a microwave beam with a width of about 10 cm; at most 10% of the molecules are in the spectrometer beam at any given time.

References

[1] R.E. Smalley, L. Wharton and D.H. Levy, Acc. Chem. Res. **10** (4), 139 (1977).
[2] T. Balle, E. Campbell, M. Keenan and W. Flygare, J. Chem. Phys. **71** (6), 2723 (1979).
[3] R. Gordon, Y. Lee and D. Herschbach, J. Chem. Phys. **54** (6), 2393 (1971).
[4] R. Larsen, S. Neoh and D. Herschbach, Rev. Sci. Instrum. **45** (12), 1511 (1974).
[5] D.P. Pullman, B. Friedrich and D.R. Herschbach, J. Chem. Phys. **93** (5), 3224 (1990).
[6] M. Gupta and D. Herschbach, J. Phys. Chem. A **105** (9), 1626 (2001).
[7] J.D. Weinstein, R. deCarvalho, K. Amar, A. Boca, B.C. Odom, B. Friedrich and J.M. Doyle, J. Chem. Phys. **109**, 2656 (1998).
[8] B.L. Lev, A. Vukics, E.R. Hudson, B.C. Sawyer, P. Domokos, H. Ritsch and J. Ye, Phys. Rev. A **77**, 023402 (2008).
[9] E. Shuman, J. Barry and D. DeMille, Nature **467**, 820 (2010).
[10] S. Ospelkaus, A. Pe'er, K.K. Ni, J.J. Zirbel, B. Neyenhuis, S. Kotochigova, P.S. Julienne, J. Ye and D.S. Jin, Nat. Phys. **4**, 622 (2008).
[11] C. Chin, R. Grimm, P. Julienne and E. Tiesinga, Rev. Mod. Phys. **82**, 1225 (2010).
[12] D. Willey, D. Bittner and F. DeLucia, J. Mol. Spectrosc. **133** (1), 182 (1989).
[13] D. Patterson, E. Tsikata and J.M. Doyle, Phys. Chem. Chem. Phys. **12**, 9736 (2010).
[14] D. Willey, R. Crownover, D. Bittner and F. DeLucia, J. Chem. Phys. **89**, 1923 (1988).
[15] D. Patterson and J. Doyle, J. Chem. Phys. **126**, 154307 (2007).
[16] W. Campbell, E. Tsikata, H.I. Lu, L. van Buuren and J. Doyle, Phys. Rev. Lett. **98**, 213001 (2007).
[17] E. Campbell, L. Buxton, T. Balle and W. Flygare, J. Chem. Phys. **74** (2), 813 (1981).
[18] G. Brown, B. Dian, K.O. Douglass, S.M. Geyer, S.T. Shipman and B.H. Pate, Rev. Sci. Instrum. **79** (5), 053103 (2008).
[19] C. Townes and A. Schawlow, *Microwave Spectroscopy* in the series *Dover Books on Physics* (Dover, New York, 1975).
[20] S. Coy, J. Chem. Phys. **73**, 5531 (1980).
[21] S. Shipman, J. Neill, B. Kroncke, B. Pate and P. Groner, *Waveguide chirped-pulse FTMW spectroscopy*, unpublished, available online at https://kb.osu.edu/dspace/bitstream/1811/33308/30/waveguide.ppt; conference presentation.
[22] M. Mengel and F.C.D. Lucia, Astrophys. J. **543** (1), 271 (2000).
[23] D. Egorov, W. Campbell, B. Friedrich, S. Maxwell, E. Tsikata, L. van Buuren and J. Doyle, Eur. J. Phys. D **31**, 307 (2004).
[24] D.R. Borst, D.W. Pratt and M. Schafer, Phys. Chem. Chem. Phys. **9**, 4563 (2007).
[25] F. Lovas and H. Hartwig, J. Mol. Spectrosc. **185** (1), 98 (1997).
[26] D. Patterson, Ph.D. thesis, Harvard University, 2010.
[27] H. Pauly, *Atom, Molecule, and Cluster Beams I* (Springer-Verlag, Cambridge, 2000).
[28] G. Scoles, *Atomic and Molecular Beam Methods* (Oxford University Press, Oxford, 1988).
[29] G.M. McClelland, K.L. Saenger, J.J. Valentini and D.R. Herschbach, J. Phys. Chem. **83** (8), 947 (1979).
[30] P. Wallraff, K. Yamada and G. Winnewisser, J. Mol. Spectrosc. **126** (1), 78 (1987).
[31] M. Schafer and A. Bauder, Chem. Phys. Lett. **308** (5–6), 355 (1999).
[32] R.V. Krems, J. Chem. Phys. **116** (11), 4517 (2002).

[33] F.J. Lovas, D.F. Plusquellic, B.H. Pate, J.L. Neill, M.T. Muckle and A.J. Remijan, J. Mol. Spectrosc. **257** (1), 82 (2009).
[34] P. Groner, E. Herbst, F.C.D. Lucia, B.J. Drouin and H. Maeder, J. Mol. Struct. **795** (1–3), 173 (2006).
[35] S.W. Stiller and M.V. Johnston, Anal. Chem. **59** (4), 567 (1987).
[36] J. Grabow, E. Palmer, M. McCarthy and P. Thaddeus, Rev. Sci. Instrum. **76**, 093106 (2005).
[37] S.T. Shipman, J.L. Neill, R.D. Suenram, M.T. Muckle and B.H. Pate, J. Phys. Chem. Lett. **2** (5), 443 (2011).
[38] J.U. Grabow, S. Mata, J.L. Alonso, I. Pena, S. Blanco, J.C. Lopez and C. Cabezas, Phys. Chem. Chem. Phys. **13** (47), 21063 (2011).
[39] C. Perez, S. Mata, S. Blanco, J.C. Lopez and J.L. Alonso, J. Phys. Chem. A **115** (34, SI), 9653 (2011).
[40] H.L. Bethlem, Ph.D. thesis, Radboud University of Nijmegen, 2002.
[41] N.R. Hutzler, H. Lu, and J.M. Doyle, preprint, abs/1111.2841 (2012). <http://arxiv.org/abs/1111.2841>
[42] M. Schnell, J.U. Grabow, H. Hartwig, N. Heineking, M. Meyer, W. Stahl and W. Caminati, J. Mol. Spectrosc. **229** (1), 1 (2005).
[43] K. Wohlfart, F. Grätz, F. Filsinger, H. Haak, G. Meijer and J. Küpper, Phys. Rev. A **77**, 031404 (2008).
[44] W. Campbell, Ph.D. thesis, Harvard University, 2008.